Interplay of phase segregation and chemical reaction: Crossover and effect on growth laws

Shubham Thwal [*] and Suman Majumder [†]
Amity Institute of Applied Sciences, Amity University Uttar Pradesh, Noida 201313, India

(Received 23 February 2024; accepted 23 May 2024; published 13 June 2024)

By combining the nonconserved spin-flip dynamics driving ferromagnetic ordering with the conserved Kawasaki-exchange dynamics driving phase segregation, we perform Monte Carlo simulations of the nearest-neighbor Ising model. This kind of mixed dynamics is found in a system consisting of a binary mixture of isomers, simultaneously undergoing a segregation and an interconversion reaction among themselves. Here, we study such a system following a quench from the high-temperature homogeneous phase to a temperature below the demixing transition. We monitor the growth of domains of both the winner; the isomer, which survives as the majority; and the loser, the isomer that perishes. Our results show a strong interplay of the two dynamics at early times, leading to a growth of the average domain size of both the winner and loser as $\sim t^{1/7}$, slower than a purely phase-segregating system. At later times, eventually the dynamics becomes reaction dominated and the winner exhibits a $\sim t^{1/2}$ growth, expected for a system with purely nonconserved dynamics. On the other hand, the loser at first show a faster growth, albeit, slower than the winner, and then starts to decay before it almost vanishes. Further, we estimate the time τ_s marking the crossover from the early-time slow growth to the late-time reaction-dominated faster growth. As a function of the reaction probability p_r, we observe a power-law scaling $\tau_s \sim p_r^{-x}$, where $x \approx 1.05$, irrespective of the temperature. For a fixed value of p_r too, τ_s appears to be independent of the temperature.

DOI: 10.1103/PhysRevE.109.064131

I. INTRODUCTION

Nonequilibrium dynamics of a system following a quench from a high-temperature disordered state to a temperature below the critical temperature T_c, marking an order-disorder phase transition, has been an active research topic over the last few decades [1,2]. Typical examples of order-disorder transitions are ferromagnetic ordering and phase segregation in a binary mixture. The equilibrium aspects of these transitions, viz., values of static critical exponents, bear universal features [3–6]. On the other hand, the corresponding nonequilibrium kinetics of the transitions may belong to different universality classes depending on the intrinsic transport mechanism of the system [7–9]. However, phenomenology of both the transitions is highlighted by the formation and growth of domains of aligned magnetic spins or like species. Importantly, the concerned domain growth is a scaling phenomenon [1,2], i.e., various morphology-characterizing functions, viz., the two-point equal-time order parameter correlation function $C(r,t)$ and the structure factor $S(k,t)$, respectively, obey the relations

$$C(r,t) \equiv \tilde{C}(x); \quad x = r/\ell(t) \tag{1}$$

and

$$S(k,t) \equiv \ell(t)^d \tilde{S}(x); \quad x = k\ell(t), \tag{2}$$

where $\tilde{C}(x)$ and $\tilde{S}(x)$ are time (t)-independent scaling functions, d is the system dimensionality, and $\ell(t)$ is the time-dependent characteristic length scale measuring the average domain size. In general, $\ell(t)$ grows in a power-law fashion as

$$\ell(t) \sim t^{\alpha}. \tag{3}$$

The growth exponent α depends on the intrinsic dynamics of the system. While for ferromagnetic ordering $\alpha = 1/2$ represents the Lifshitz-Cahn-Allen (LCA) law [10], for a solid binary-mixture phase segregation $\alpha = 1/3$ stands for the Lifshitz-Slyozov (LS) law [11,12].

In ferromagnetic ordering or phase ordering, typically one starts with a system having magnetization $m \approx 0$, and after the quench the system approaches its new equilibrium state where $m \neq 0$. The intrinsic dynamics of this phenomenon is nonconserved, as the order parameter m changes continuously during the evolution. Conversely, during phase segregation in a binary mixture following a quench from a homogeneous or miscible phase, the order parameter, i.e., the concentration difference χ between the two species, remains constant throughout the evolution. Thus, its dynamics is said to be conserved. Monte Carlo simulations (MC) of the nearest-neighbor Ising model have been used extensively to study domain growth in both conserved and nonconserved systems, and the corresponding growth laws have been verified [1,13–17]. Recently, the interest has shifted toward investigating domain growth in more complex and computationally demanding systems, e.g., the long-range Ising model with power-law interaction, using both conserved and nonconserved order-parameter dynamics [18–21].

In this paper, by means of MC simulations of the Ising model, we investigate the effects of combining conserved and nonconserved dynamics on the domain-growth laws. The motivation of studying such a system stems from understanding the nonequilibrium dynamics of a binary mixture where

[*]Contact author: shubhamthwal1@gmail.com
[†]Contact author: smajumder@amity.edu; suman.jdv@gmail.com

an interconversion reaction among the components occurs simultaneously with segregation among themselves. A typical example of such a system undergoing interconversion reaction is isomeric mixtures, e.g., conversion of cis-isomer to trans-isomer or conversion between optical isomers or enantiomers [22]. Either naturally or due to some external drive, the components of the isomeric mixture do segregate from each other, and in combination with the interconversion reaction the mixture gets enriched with one of the isomers [23–30]. Apart from the segregation of the reacting isomeric mixture, such a simultaneous presence of both segregation and reaction dynamics can effectively explain the collective dynamics of cell-adhesion bonds [31] and opinion-based segregation of social groups [32] using the Schelling model [33]. Numerical simulations based on a similar foundation has also been successfully employed to explore the dynamics of chemically active droplets whose segregation is vital to structure the interior of the biological cell [34–36].

There have been a few studies on phase segregating reacting binary isomeric mixtures either by using MC simulations of the Ising model or by solving the corresponding Cahn-Hilliard-Cook (CHC) equation [37–41]. While most of these studies were motivated to understand the amplification of one of the phases, the CHC approach focused on the domain-growth laws reporting a crossover from an early-time reaction controlled LCA behavior to a late-time diffusion controlled LS behavior [40]. Interest has also been laid on considering reactions in solution via molecular dynamics (MD) simulations [42]. Even studies with forceful preservation of the compositions being imposed along with the interconversion reaction have also been conducted, leading to fascinating pattern formation mimicking morphology of microphase separation found in the biological world [43]. Lately, using the Ising model, it has been shown that the Arrhenius behavior of the interconversion reaction gets significantly affected due to the simultaneous existence of the segregation process [44]. Technically, studies of these systems using MC simulations of the Ising model is done by mixing two types of dynamics, i.e., the nonconserved spin-flip Glauber dynamics [45] and the conserved spin-exchange Kawasaki dynamics [46].

The effective dynamics of the system described above is nonconserved, i.e., in the final state one of the reacting species will survive as the majority which we refer to as the winner and the other one as loser. Recently, one of us demonstrated how to disentangle the growth of the winner from the loser during phase ordering [47]. Importantly, such a disentanglement allows one to realize the scaling laws associated with domain growth using systems with relatively smaller size. Here, adopting the same disentanglement protocol, we study the growth of the winner and loser in a binary mixture of isomers which is undergoing both segregation and an interconversion reaction. This not only allows us to have an appropriate realization of the associated domain-growth laws but also to extract a timescale that marks the crossover between the two types of dynamics present in the system.

The rest of the paper is arranged in the following manner. In the next section, we present details of the model we used and an elaborate description of the performed MC simulations. Following that, in Sec. III we present the results and wherever required also describe the calculations of relevant observables. Finally, we conclude in Sec. IV by providing a brief summary and a future outlook.

II. MODEL AND METHOD

To model a binary isomeric mixture ($A_1 + A_2$) undergoing interconversion reaction, we use the nearest-neighbor Ising model having the Hamiltonian

$$H = -J \sum_{\langle ij \rangle} S_i S_j, \tag{4}$$

where the spin $S_i = +1(\text{or } -1)$ represents the component $A_1(\text{or } A_2)$ of the mixture, and J is the strength of interaction. The sign $\langle \dots \rangle$ denotes that only nearest-neighbor interactions are considered. We consider our system to be a square lattice ($d = 2$) having a linear dimension L, and apply periodic boundary condition (PBC) in all directions. The Ising model in a square lattice with PBC undergoes a phase transition with a critical temperature [48]

$$T_c = \frac{2J}{k_B \ln(1+\sqrt{2})}, \tag{5}$$

where k_B is the Boltzmann constant. For a binary mixture, the critical temperature is equivalent to the demixing transition temperature.

We consider that the components are undergoing the following interconversion reaction:

$$A_1 \rightleftharpoons A_2. \tag{6}$$

At the same time, they are also spontaneously segregating from each other, for which the energetics is captured by the Hamiltonian in Eq. (4). As already mentioned, we perform MC simulations of the above model where one needs to incorporate the dynamics of both processes. The dynamics of the interconversion reaction in Eq. (6) is effectively mimicked by the Glauber spin-flip move, used for capturing the nonconserved dynamics of phase ordering [45,49,50]. There one randomly picks up a spin on the lattice and flips it upside down. The dynamics of segregation between the components is introduced via the Kawasaki spin-exchange move, typically used for simulating phase segregation, where the dynamics is conserved [46,49,50]. In this move, one randomly picks up a pair of nearest-neighbor spins and exchanges their positions. In our simulations, we attempt both moves and accept them using the Metropolis criterion with the probability [49,50]

$$p_i = \min[1, \exp(-\Delta E/k_B T)], \tag{7}$$

where ΔE is the change in energy due to the attempted move and T is the temperature. For convenience, we choose $k_B = 1$.

As the initial condition for our simulation, we prepare a homogeneous 50:50 binary mixture of A_1 and A_2 by placing them randomly on the lattice sites. This mimics a high-temperature disordered state. We then set the temperature to $T < T_c$ in our simulations, where we also introduce a relative weightage between the nonconserved and conserved moves using a parameter called the reaction probability p_r. It denotes the probability of attempting the Glauber spin-flip move at each MC step. Thus, the Kawasaki spin-exchange attempt is performed with a probability $1 - p_r$. We perform simulations for a range of values of $p_r \in [10^{-4}, 10^{-1}]$. We choose the unit

of time to be one MC sweep (MCS), which corresponds to L^2 attempted MC moves. In our simulations, J sets the unit of energy and J/k_B the unit of temperature. All the results are for a system with $L = 128$ containing $L^2 = 16\,384$ number of spins or isomers. All the simulations are run until 10^7 MCS, which is sufficient to extract meaningful results for the chosen system size considering the covered variations of T and p_r. Except for the time evolution snapshots, all subsequently presented results are averaged over 20 independent initial configurations, obtained by using different seeds in the random number generator. Given that the system size is rather large, the use of a statistically small number of independent realizations is sufficient for our study. This is due to the self-averaging nature of the primary quantity of interest, i.e., the average domain size.

In the past, nonequilibrium dynamics of systems with such mixed dynamics have been studied reasonably well in a slightly different context [51–56]. In these studies, an athermal Kawasaki-exchange move was introduced along with the spin-flip moves in a magnetic system. The athermal Kawasaki-exchange move takes into account an energy flux into the system while the Glauber dynamics simulates the contact of the system with the a heat bath. This leads to a different class of nonequilibrium steady states than what is considered here.

III. RESULTS

In this section, we present our main results. It is further divided into two subsections. In the first subsection, we deal with simulation results at a fixed temperature $T = 0.5T_c$. In the second, we present results obtained for a variation of T.

A. Dynamics at $T = 0.5T_c$

Here we present results for a fixed quench temperature $T = 0.5T_c$. The effect of slow dynamics at low T and difficulty of estimating various observables at high T due to thermal noise are negligible at such a moderate T. In Figs. 1(a)–1(d), we present time-evolution snapshots for different reaction probabilities p_r. As expected, the time evolution at the largest p_r, shown in Fig. 1(a), bears almost a perfect resemblance with time evolution during ferromagnetic ordering. There one can hardly notice any effect of phase segregation as the dynamics of the chemical reaction dominates throughout the evolution, and one eventually ends up with one of the isomers as the majority or winner, equivalent to the final magnetized state obtained during ferromagnetic ordering. As p_r decreases, gradually the effects of phase segregation show up. For $p_r = 10^{-3}$ and 10^{-4}, one can clearly notice the bicontinuous domain morphology at early times, a classic signature of spinodal decomposition in a phase-segregating system [13,15,16]. Eventually, the reaction takes over at later times and the system approaches toward a state where one of the isomers emerges as the winner. For very small p_r, this dynamics slows down as one can appreciate from the snapshot shown at the latest time for $p_r = 10^{-4}$. Since the focus of this paper is on the domain-growth laws and its crossover dynamics, here we do not explore the kinetics of the interconversion reaction and rather refer to Ref. [44] for that.

It is clear from the time evolution snapshots that the pattern morphologies while the system is evolving is affected by the two competing dynamics. As a first check, we calculate the two-point equal-time correlation function,

$$C(r,t) = \langle S_i S_j \rangle - \langle S_i \rangle \langle S_j \rangle, \tag{8}$$

where $r = |i - j|$ is the distance between the spins at lattice sites i and j, and $\langle \dots \rangle$ indicates averaging over all the sites. Following the traditional approach [1,2,40], we extract the average domain length $\ell(t)$ using the criterion

$$C[r = \ell(t), t)] = \tfrac{1}{2}C(0,t). \tag{9}$$

Using this $\ell(t)$, in Figs. 2(a)–2(d) we plot $C(r,t)$ against the scaled variable $r/\ell(t)$ at different times to verify the scaling quoted in Eq. (1) for different values of the reaction probability p_r. For the largest p_r, presented in Fig. 2(a), we obtain a reasonably good collapse of data for different times until the finite-size effect is experienced at $t \approx 10^4$. Such a behavior is expected for ferromagnetic ordering. As p_r decreases, one notices that in Fig. 2(b) the data collapse is reasonable only for intermediate times. Absence of data collapse for $t = 10$ and 10^2 suggests that the system is still under the effect of phase segregation. At the latest time, the data again are affected by the finite size of the system. With further decrease of p_r, the data in Figs. 2(c) and 2(d) show reasonably good collapse until $t = 10^4$, however, with an oscillating behavior around zero at large r, typical of conserved dynamics of phase segregation. Note that since the dynamics for very small p_r is slow, the system is not expected to experience any finite-size effects until $t \approx 10^5$. Thus, the noncollapsing behavior of the data at $t = 10^5$ in Figs. 2(c) and 2(d) can only be attributed to the dominance of the interconversion reaction. In all cases, the dip of $C(r,t)$ to small negative values at large $r/\ell(t)$, i.e., at r beyond the average domain length is due to the alternate presence of domains of different species (see Fig. 1) as one moves across the lattice.

The scaling behavior in the kinetics can be also probed by another quantity, i.e., the structure factor which is determined by the Fourier transform:

$$S(\mathbf{k},t) = \int d\mathbf{r} C(\mathbf{r},t) e^{i\mathbf{kr}}. \tag{10}$$

In Figs. 3(a)–3(d), we verify the scaling of $S(k,t)$, embedded in Eq. (2). Like the data for $C(r,t)$, for $p_r = 10^{-1}$ the behavior of $S(k,t)$ in Fig. 3(a) is reminiscent of a typical ferromagnetic ordering. However, with decreasing p_r, the data presented in Figs. 3(b)–3(d) show reasonably good collapse, i.e., the data cannot unambiguously capture the interplay of the conserved phase segregation dynamics and the nonconserved dynamics due to the interconversion reaction. Noticeable is, of course, the power-law behavior of the tail, independent of time and p_r. The dashed lines in Fig. 3 show the consistency of this power-law decay with the generalized Porod law for scalar order parameter given as [57,58]

$$S(k,t) \sim k^{-(d+1)}. \tag{11}$$

Here the power-law exponent is $d + 1 = 3$, mentioned next to the dashed lines. Thus, it seems that the Porod-tail behavior is unaffected by the interplay of the two dynamics. The Porod law was originally derived in the general context of scattering

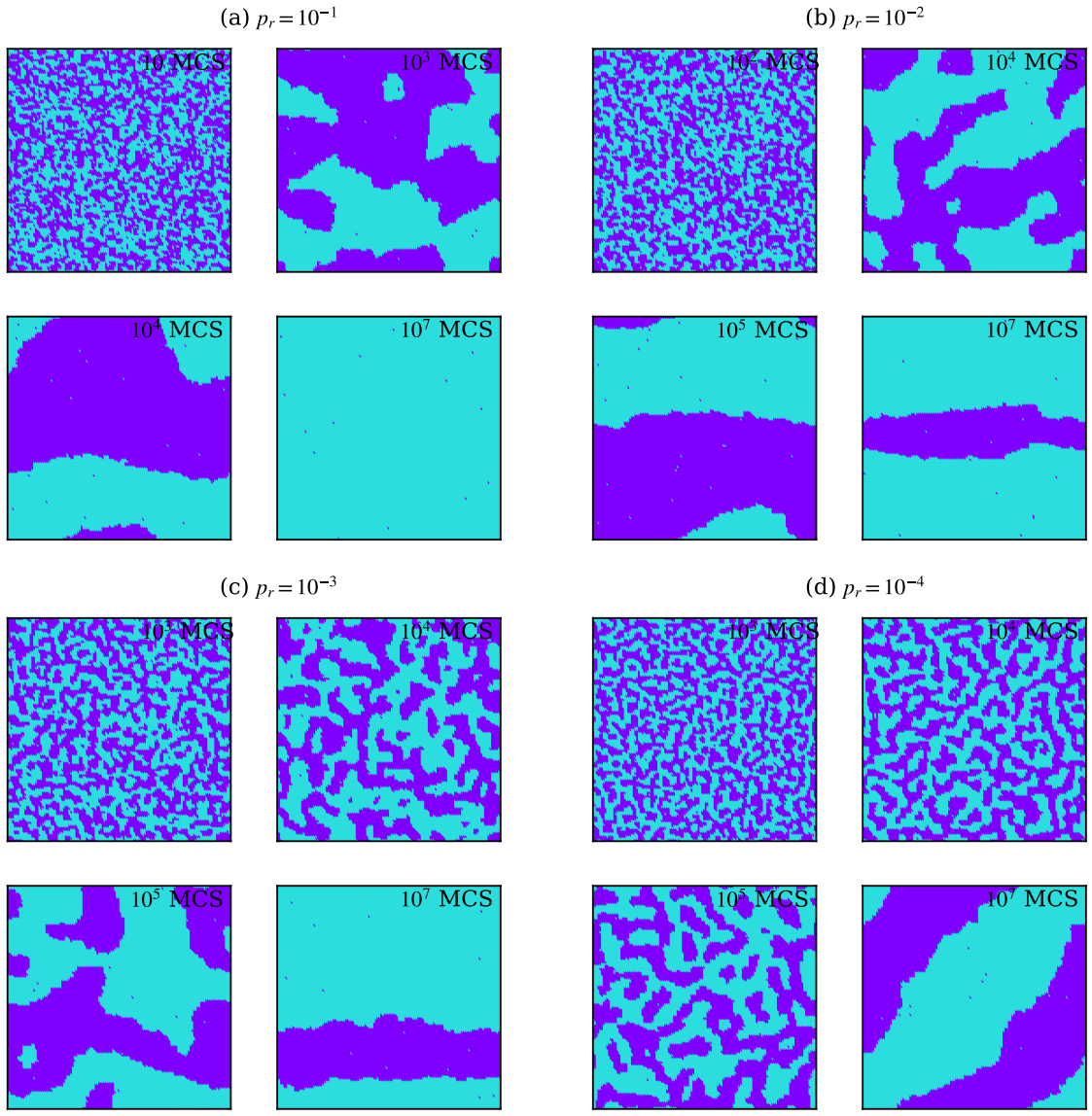

FIG. 1. Snapshots at different times representing the evolution of a binary mixture of isomers ($A_1 + A_2$), where an interconversion reaction is occurring simultaneously with segregation. The initial system is a homogeneous 50:50 mixture of the two isomers in a square lattice of linear dimension $L = 128$, mimicking a configuration above the critical temperature T_c, which is then quenched to a temperature $T = 0.5T_c$. Results are presented for different values of the reaction probability p_r, as indicated. The two colors correspond to the location of the two different isomers on the lattice.

from two-phase media [57,58]. Later, it was shown that for an ordering system, it originates from the short-distance singularities [1], i.e., for $k\ell \gg 1$. There, the solely presence of sharp interfaces was assumed, and for $k\ell \gg 1$ it was considered that *S(k, t)* should scale as the total volume of the defect core. Given that in $d = 2$ for scalar order parameter the defect dimension is 1, the amount of defect per unit volume scales as ℓ^{-1}. Extracting this factor from the general scaling relation in Eq. (2), one arrives at $S(k,t) \sim \ell^{-1}k^{-3}$, the Porod law. Since the basic assumption of the sharp interface presence is independent of the dynamics, the Porod law has been realized individually for both the conserved and the nonconserved Ising model [2]. Hence, it holds true even for a system with mixed dynamics.

Next, we move on to explore the interplay of dynamics via the time dependence of the growing sizes of the domains. As shown previously by one of us that disentanglement of the kinetics of the winner from the loser allows one to realize the growth laws unambiguously, here also we rely on the same [47]. Thus, rather than using the average domain size $\ell(t)$, at a given time we estimate the average domain size $\ell_1(t)$ of the winner and also $\ell_2(t)$ of the loser. For details on how these lengths are estimated, we refer to Ref. [47]. The measured domain lengths of the winner for different p_r are presented in Fig. 4(a) on a double-log scale. The data for $p_r = 10^{-1}$ show a single growth regime, consistent with a $\ell_1(t) \sim t^{1/2}$ power-law behavior, i.e., the LCA law. The flat behavior following the power-law growth indicates that finite-size effects have started showing up. At even later times, one sees a jump that corresponds to an avalanche [47,59]. As p_r decreases, an initial regime with a much slower growth emerges by virtue of the dominance of phase segregation dynamics over the

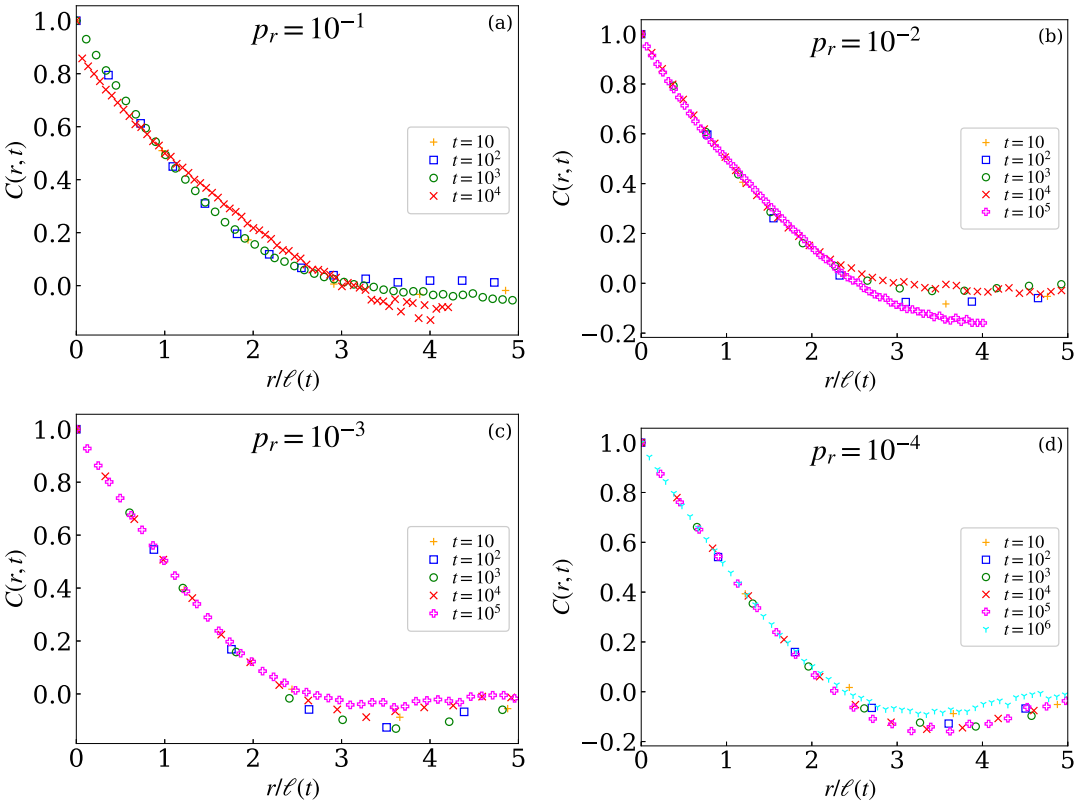

FIG. 2. Plots of the two-point equal-time correlation function $C(r,t)$ as a function of the scaling variable $r/\ell(t)$ at different times for different values of the reaction probability p_r, as indicated. Here, the average domain length $\ell(t)$ is calculated from the crossing of the unscaled data of $C(r,t)$, using the condition prescribed in Eq. (9). See text for details. All results are at a temperature $T = 0.5T_c$ for a system of size $L = 128$.

interconversion reaction dynamics. At later times, one sees again a growth consistent with the LCA law. The duration of the initial slow regime gets extended as p_r decreases. In fact, for $p_r = 10^{-4}$, within the given maximum simulation time, the slowest regime appears to be longer lived. The data for $p_r = 10^{-3}$ follow the data for $p_r = 10^{-4}$ until $t \approx 500$, when the reaction dynamics takes over. For $p_r = 10^{-4}$ the data continue to grow slowly, consistent with a $\ell_1 \sim t^{1/7}$ behavior, which is much slower than the expected LS behavior $\ell_1 \sim t^{1/3}$ for a phase-segregating system. This implies that the growth of the domains slows down significantly in the presence of an interconversion reaction. On the other hand, when the domains of the two isomers are well separated, phase segregation seizes and the dynamics is entirely controlled by the interconversion reaction. Hence, at late times the LCA behavior is always realized, as shown by the data for all p_r.

In Fig. 4(b), we show the time dependence of the average domain size $\ell_2(t)$ of the loser for different p_r. There also, for $p_r = 10^{-1}$ one sees a single growth regime followed by a plateau before it suddenly vanishes due to the avalanche effect, also observed as a corresponding abrupt increase of $\ell_1(t)$ in Fig. 4(a). In the power-law regime, the growth is consistent with $\ell_2(t) \sim t^{0.45}$, albeit slower than what is observed for the corresponding $\ell_1(t)$. With decreasing p_r a slower early-time regime emerges like in the time dependence of $\ell_1(t)$. Here, also, the early-time regime gets extended as p_r decreases. For $p_r = 10^{-4}$, the growth in this early-time regime is consistent with a $\ell_2(t) \sim t^{1/7}$ behavior, similar to what is observed for the corresponding $\ell_1(t)$ in Fig. 4(a). This indeed confirms that in this early-time regime the dynamics is controlled by the phase segregation, however, the occurrence of the interconversion reaction every now and then makes the dynamics slower than the LS growth, expected for an ideal phase-segregating system. For smaller p_r the very late-time behavior is not observed within the given maximum simulation time. Overall, from the plots presented in Figs. 4(a) and 4(b), we infer that, during the evolution, initially the phase segregation is dominant with occasional involvement of the interconversion reaction, and thus the growth of the domains of the isomers in this regime is even slower than LS law. However, at later times phase segregation is no more capable of driving the system, as either the system has completely phase segregated or the domains of the individual isomers are very well separated. Hence at reaction-dominated late times, the dynamics is perfectly consistent with the LCA law, expected for ferromagnetic ordering.

The other important aspect of the kinetics is, of course, the timescale when the system crosses over to the reaction dominated regime. This crossover is more clearly visible if one plots the time dependence of the difference between the domain length of the winner and loser, i.e., $\ell_1 - \ell_2$, as presented in Fig. 4(c) for the data in Figs. 4(a) and 4(b). In this case, the behavior is almost similar for all p_r. Initially, for a certain period, $\ell_1 - \ell_2$ remains constant followed by a steady

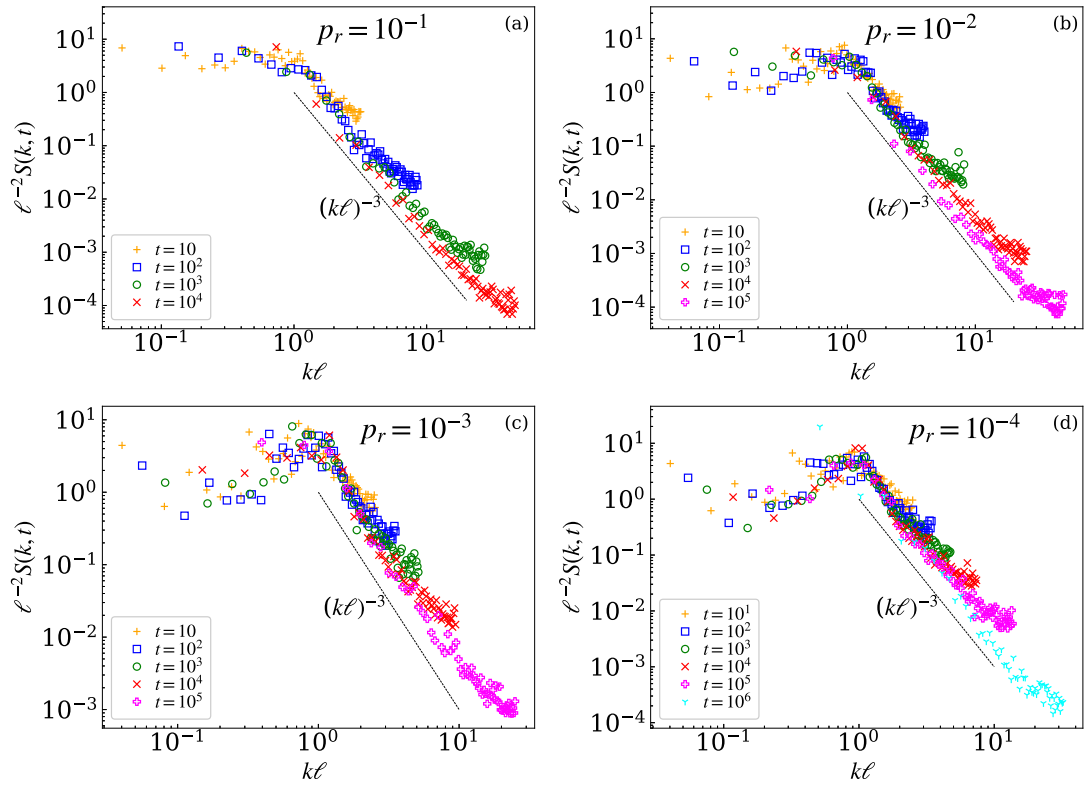

FIG. 3. Scaling plots of the structure factor $S(k,t)$ at different times for different values of the reaction probability p_r, as indicated. Here also, the average $\ell(t)$ used is obtained from $C(r,t)$. The dashed line at large k represents the Porod tail. The results are for the same systems as presented in Fig. 2.

growth consistent with the solid line representing

$$\ell_1 - \ell_2 \sim t, \tag{12}$$

i.e., linear behavior with time. It can be easily noticed that the time when the flat behavior of $\ell_1 - \ell_2$ switches over to a linear growth shifts toward the right with decrease in p_r. From this time onward, the growth of ℓ_1 is significantly faster than the corresponding growth in ℓ_2, thus indicating a crossover to the reaction dominated dynamics. Based on this observation, we define the crossover time τ_s from segregation to reaction dominated regime such that it satisfies the relation

$$\ell_1(\tau_s) - \ell_2(\tau_s) = \eta, \tag{13}$$

where η prescribes how much difference between ℓ_1 and ℓ_2 is considered. Finding out the inflection point where the data in Fig. 4(c) change from a roughly constant behavior to a linear scaling would have been a more natural estimate for the crossover time. However, a close look at Fig. 4(c) reveals that for smaller p_r in the segregation dominated region, $\ell_1 - \ell_2$ is not really constant. Hence, technically it would be ambiguous to determine the inflection point. On the other hand, a proper choice of η in Eq. (13) provides a consistent estimate of the crossover time.

In Figs. 5(a)–5(c), we show the plots of τ_s as a function of p_r for three different choices of the parameter η in Eq. (13). There the errors are estimated from a Jackknife analysis, where τ_s is calculated independently for each Jackknife bin that contains all but data from one of the 20 initial realizations we used [60]. The apparent linear behavior of the data on a double-log scale implies a power-law dependence of τ_s on p_r. To quantify this power-law behavior we write the following ansatz:

$$\tau_s = A p_r^{-x}, \tag{14}$$

where A is a prefactor and x is the power-law exponent. We fit this ansatz to our data, the results of which are tabulated in Table I. In Figs. 5(a)–5(c), the dashed lines represent the obtained best fits. The results suggest that although the prefactor A increases with η, the estimated exponent $x \approx 1.07$ is very weakly dependent on the choice of η. Hence, for all subsequent estimations of τ_s we rely only on the choice $\eta = 1$.

B. Temperature dependence of the dynamics

In this subsection, we investigate the temperature dependence of the kinetics. For that purpose, we perform simulations for different values of the reaction probability p_r at different temperatures below T_c.

Here, we do not present the time evolution snapshots for different temperatures, and rather straight away move on to the time dependence of the average domain sizes. We start with plots of the average domain size $\ell_1(t)$ of the winner in Fig. 6 for five different temperatures. For the largest reaction probability, i.e., $p_r = 10^{-1}$, presented in Fig. 6(a), the growth of $\ell_1(t)$ consists of a single regime for all T. At moderate temperatures, i.e., $T = 0.4T_c$, $0.5T_c$, and $0.6T_c$, this growth seems to be consistent with the LCA law $\ell_1 \sim t^{1/2}$. However, for higher T, a significant deviation from the LCA law is

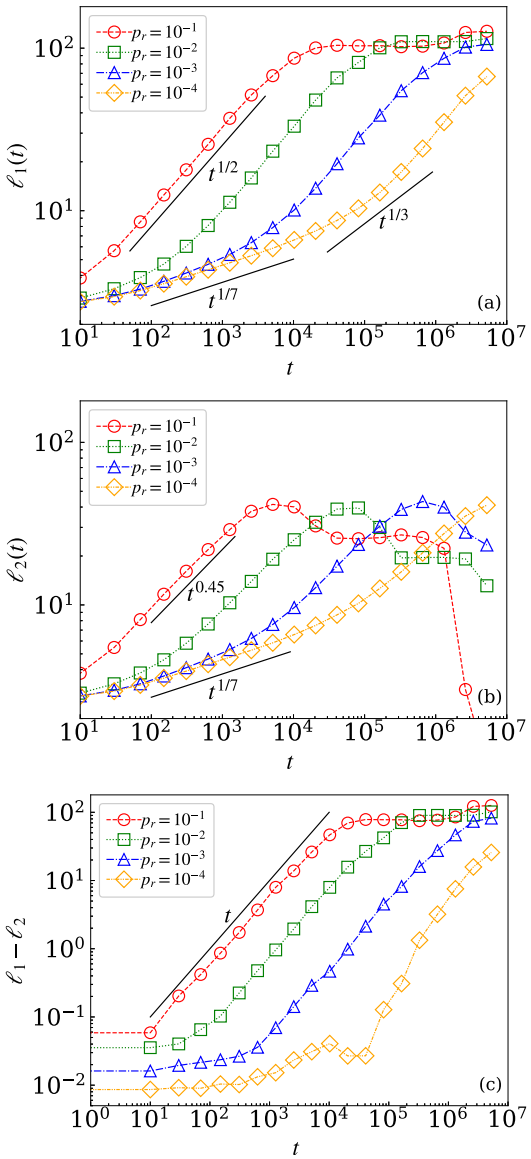

FIG. 4. Double-log plots of the time dependence of the average domain size (a) of the winner $\ell_1(t)$ and (b) the loser $\ell_2(t)$, for different reaction probabilities p_r, obtained from simulations using a system of size $L = 128$ at $T = 0.5T_c$. In (c), we show the corresponding time dependence of the difference $\ell_1 - \ell_2$, for different p_r. The solid lines in all panels represent different power-law behaviors as mentioned next to them.

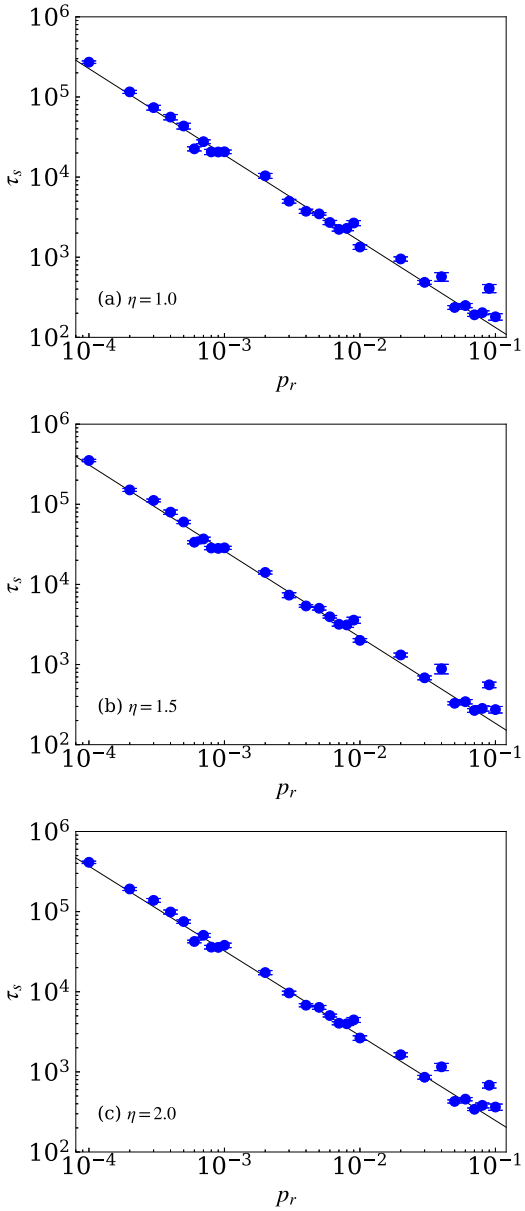

FIG. 5. Double-log plots of the crossover time τ_s as a function of the reaction probability p_r, at $T = 0.5T_c$ using a system of size $L = 128$, for different choices of the parameter η in Eq. (13). The dashed lines are the best fits obtained using the ansatz in Eq. (14). For details, see the main text.

observed as the growth becomes slower with increase in T. The inconsistency of the data with the other solid line implies that the slow growth is certainly faster than the LS growth $\ell_1(t) \sim t^{1/3}$. Also, at high T there is no chance of dynamic freezing [61]. Thus, the apparent slow growth can be attributed to the presence of significantly large noise clusters at high T that do not allow estimation of $\ell_1(t)$ from a pure domain morphology of the winner. This reasoning can further be appreciated from the fact that at very late times when the reaction has almost finished, $\ell_1(t)$ is supposed to be saturated at a value $\approx L$, at high T this happens at $\ell_1(t) < L$. This problem can of course be tackled by appropriate noise removal technique [15–17]. Nevertheless, we abstain ourselves from doing so and rather stress that the observation of a single growth regime independent of T suggests a reaction-dominated dynamics for $p_r = 10^{-1}$ at all T.

TABLE I. Fitting results for τ_s vs p_r data presented in Fig. 5, using the ansatz in Eq. (14).

η	A	x
1.0	11.12 ± 1.1	1.08 ± 0.02
1.5	15.53 ± 1.6	1.08 ± 0.02
2.0	21.63 ± 2.1	1.06 ± 0.02

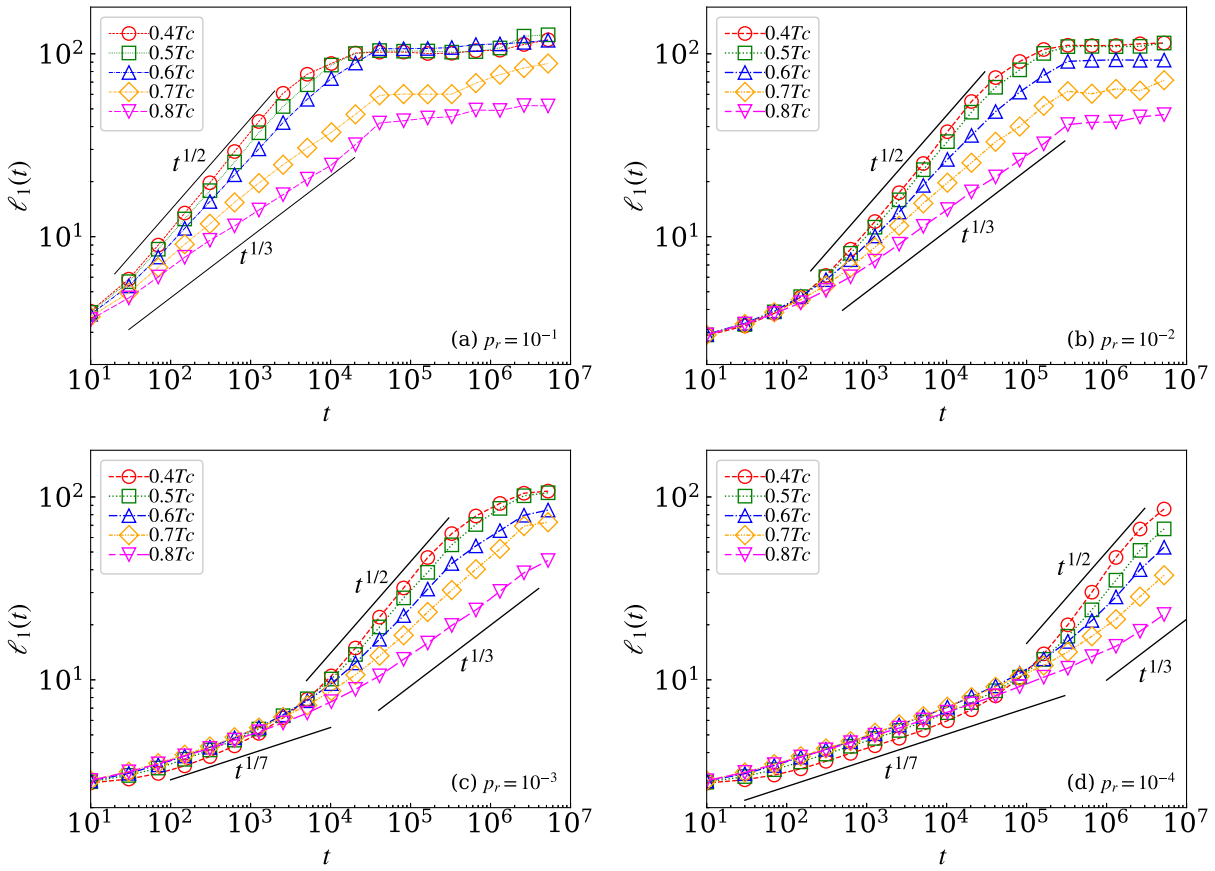

FIG. 6. Double-log plots of the time dependence of the average domain size of the winner $\ell_1(t)$ at different temperatures for different reaction probability p_r, using a system of size $L = 128$. The two solid lines representing power laws $\ell_1 \sim t^{1/2}$ and $\ell_1 \sim t^{1/3}$ are, respectively, the LCA and LS growths. In (c) and (d), an additional solid line representing the power-law $\ell_1 \sim t^{1/7}$ is also shown for the initial growth regime.

As p_r decreases, one can clearly see the emergence of an initial slow-growth regime for $\ell_1(t)$ at all temperatures. As shown in Fig. 6(b), for $p_r = 10^{-2}$ the initial slow-growth regime is very short-lived as there still the reactions start to control the dynamics from early time. Followed by the slow growth, $\ell_1(t)$ shows a faster growth that is again consistent with the LCA law at moderate temperatures. Again, for higher temperatures the growth, although faster than the LS growth, is apparently significantly slower than the LCA law which again could be attributed to the effect of noisy clusters while estimating $\ell_1(t)$.

For even smaller p_r, presented in Figs. 6(c) and 6(d), the initial slow regime of $\ell_1(t)$ is long-lived and prominent. Consistency of the data at all T with the power-law behavior $\ell_1 \sim t^{1/7}$ suggests its robustness. At later times, the data cross over to a faster growth when the dynamics is dominated by the interconversion reaction. The growth then again is consistent with the LCA law for moderate T. At high T, for both $p_r = 10^{-3}$ and 10^{-4} the data again show significant deviation from the LCA law. For $p_r = 10^{-4}$ at $T = 0.8T_c$, the data even seem to be consistent with a $\ell_1(t) \sim t^{1/3}$ behavior. However, we stress that this is just a mere coincidence and should not be treated as the realization of the LS behavior. In fact, this slow growth at late times, as already mentioned, is an artifact of the estimation of $\ell_1(t)$ from impure domain morphology at high T.

The temperature dependence of the average domain size of the loser $\ell_2(t)$ corresponding to the cases discussed above are presented in Fig. 7. For the largest value of $p_r = 10^{-1}$, shown in Fig. 7(a), the comparative behavior among different T is similar to what is observed for $\ell_1(t)$ in Fig. 6(a). At the lowest T, the data are consistent with the LCA law. At later times, the data show a flat behavior before they eventually decay and almost vanish. As T increases, the behavior is similar, except for the fact that the growth becomes slower, which again is due to the fact that the estimated $\ell_2(t)$ is not from a pure domain morphology. Noticeable is that the time taken by $\ell_2(t)$ to almost vanish, decreases as T increases. This is a signature of the fact that for $p_r = 10^{-1}$, the total reaction time or kinetics of the reaction follows an Arrhenius behavior [44].

The behavior of the data for $p_r = 10^{-2}$, presented in Fig. 7(b), is similar to what is observed for $p_r = 10^{-1}$. At low T, in the growth regime, again the data are almost consistent with the LCA law and deviate significantly as T increases. Following a brief period of flat behavior, $\ell_2(t)$ start to decay and almost vanish at late times. The trend of the data again indicates an Arrhenius behavior. With further decrease of p_r, within the growth regime there exists two subregimes as shown by the plots presented in Figs. 7(c) and 7(d), like what is observed for $\ell_1(t)$ in Figs. 6(c) and 6(d). The initial slow-growth regime here is consistent with the power law $\ell_2(t) \sim t^{1/7}$, similar to how $\ell_1(t)$ behaves. This confirms that,

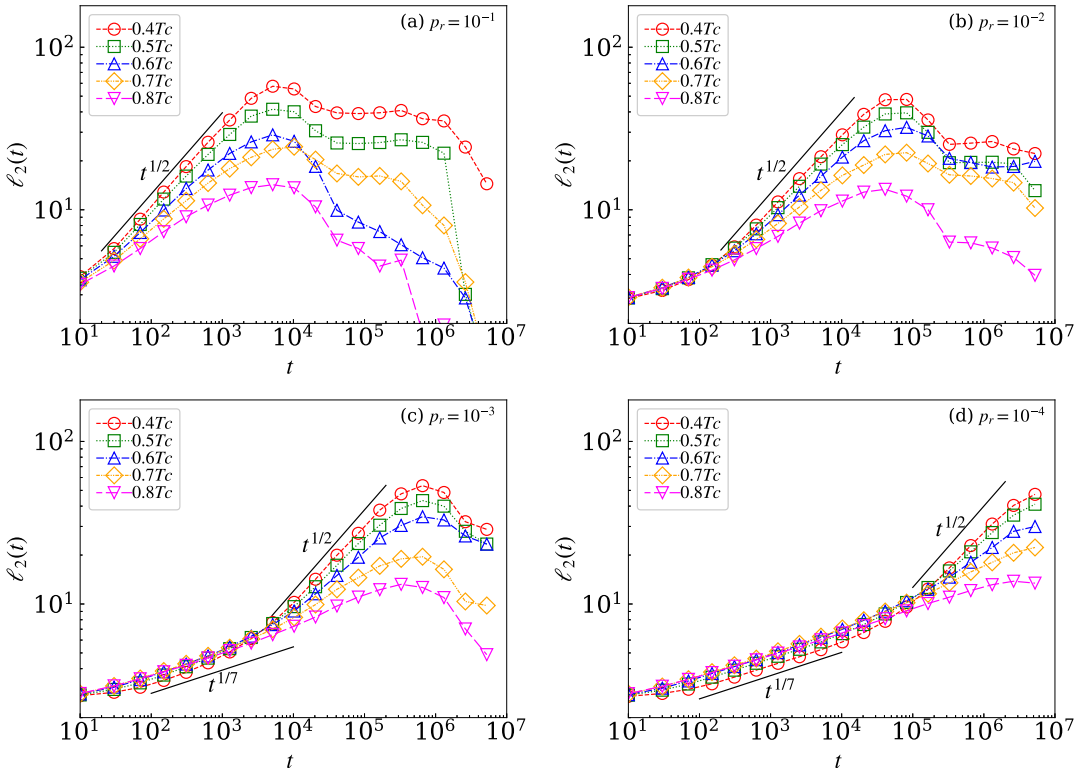

FIG. 7. Double-log plots of the time dependence of the average domain size of the loser $\ell_2(t)$ at different temperatures for different reaction probability p_r, using a system of size $L = 128$. The solid line representing the power law $\ell_2 \sim t^{1/2}$ is for the LCA growth. In (c) and (d), the initial growth regime of $\ell_2(t) \sim t^{1/7}$ is also shown as a solid line.

irrespective of T, when the reaction probability p_r is small, initially the dynamics is almost conserved due to the dominant effect of segregation, however, it is much slower than the LS growth. At later times when the interconversion reaction starts to dominate, the growth becomes faster for a brief period, albeit slower than the LCA growth, before eventually starting to decay. Within the maximum simulation time of 10^7 MCS, for $p_r = 10^{-3}$ and 10^{-4} the data for $\ell_2(t)$ do not reach the point where they almost vanish. Hence, from this data it is not possible to infer anything about the Arrhenius behavior of the interconversion reaction. In this regard, we refer to Ref. [44], where it has been shown that for lower p_r values, the Arrhenius behavior of the interconversion reaction gets disrupted.

In the segregation dominated regime, naively, one would expect that the power-law exponent should sit somewhere between $1/3$ and $1/2$. Results at different T clearly confirm that is not the case, for which we provide the following heuristics. For low p_r, it is expected that the dynamics is dominated by the Kawasaki-exchange moves. However, occasionally some Glauber spin-flip moves also get accepted. Once the domains are considerably big in size, the growth due to segregation occurs via merging of domains. The occasional Glauber moves disrupt this merging of domains by flipping the spins connecting the big domains when they are slightly in contact with each other, as illustrated in the upper panel of the schematic in Fig. 8. Energetically, this is more likely than flipping of the in-between spins of two approaching domains (shown in the lower panel of Fig. 8) to enhance the growth by connecting them. Hence, instead of having a growth exponent somewhere between $1/3$ and $1/2$, one ends up getting $1/7$, smaller than the LS exponent. Nevertheless, an appropriate theoretical understanding is needed to further substantiate this heuristics and the exact value of the observed exponent.

Now we move on to investigate the effect of temperature on the crossover time τ_s that marks the switchover to a completely reaction dominant dynamics. As already mentioned, τ_s is calculated using the prescription embedded in Eq. (13) with $\eta = 1$. In Fig. 9(a), we show the plots of the τ_s as a function of p_r, at different T. All the data seem to be parallel to each other except for the data points at $p_r = 10^{-1}$ for $T = 0.7T_c$ and $0.8T_c$. Possibly, the crossover is not so sharp at high T, as

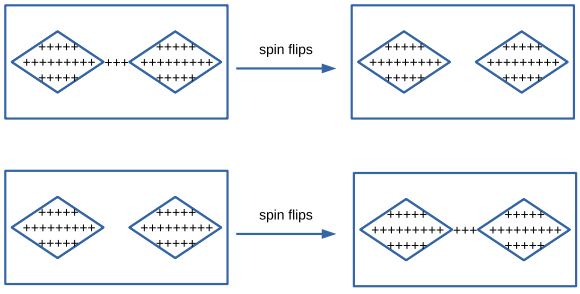

FIG. 8. Schematic representing the heuristics to explain the early-time slow growth of domains in the segregation dominated regime. The upper panel shows the likely spin-flip events where two adjacent domains get detached from each other and thereby slow down the domain growth compared to the LS growth. The lower panel depicts the unlikely spin-flip events speeding up the growth by merging of two approaching domains.

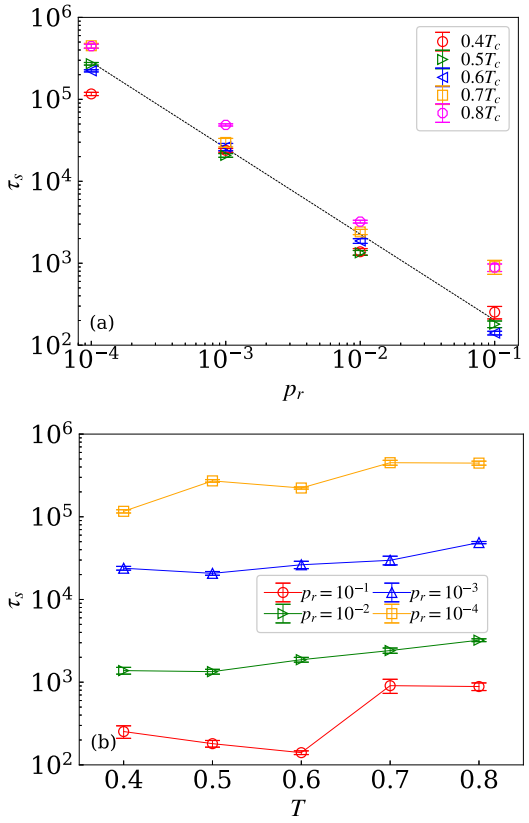

FIG. 9. (a) Double-log plots of the crossover time τ_s as a function of the reaction probability p_r at different T using a system of size $L = 128$. The dashed line represents Eq. (14) with $A = 17.97$ and $x = 1.05$. (b) Variation of τ_s as a function of T, for fixed p_r as mentioned.

the rate of both phase segregation and interconversion reaction get enhanced due to huge thermal fluctuations. Hence, the criterion used in Eq. (13) fails to unambiguously extract the crossover time τ_s. Nonetheless, we obtain reasonable results when we fit the ansatz in Eq. (14) to the data at different T, the results of which are tabulated in Table II. From the values quoted there, we calculate the average prefactor $A = 17.97 \pm 3.1$ and $x = 1.05 \pm 0.07$, which, of course, have significant error bars. Nevertheless, in Fig. 9(a) we plot a dashed line representing Eq. (14) with the above quoted values. The data indeed look more or less parallel to the dashed line except for the points representing $p_r = 10^{-4}$ at $T = 0.7T_c$ and $0.8T_c$.

The variation of τ_s with T for fixed values of the reaction probability p_r are shown in Fig. 9(b). The almost flat behavior of the data for all cases indicate that the crossover is very weakly dependent on the temperature, although for a purely segregating system it has been shown that the relaxation time shows an Arrhenius behavior [44]. This, of course, is courtesy of the effect of the presence of interconversion reaction even when the dynamics is dominated by segregation.

TABLE II. Fitting results for τ_s vs p_r data at different temperatures using the ansatz in Eq. (14).

T	A	x
$0.4T_c$	26.54 ± 18.8	0.92 ± 0.08
$0.6T_c$	12.74 ± 1.7	1.06 ± 0.02
$0.7T_c$	13.64 ± 6.4	1.13 ± 0.06
$0.8T_c$	25.81 ± 12.8	1.07 ± 0.07

IV. CONCLUSION

To summarize, we have presented results on the effects of interplay of phase segregation and interconversion reaction on the kinetics of domain growth. For that purpose, we have performed Metropolis MC simulations of the nearest-neighbor Ising model in a square lattice, governed by both conserved and nonconserved dynamics. The system mimics a phase-segregating isomeric binary mixture. Starting from such a homogeneous binary mixture, we have studied the nonequilibrium kinetics when the system is quenched below the demixing or critical temperature. Due to the presence of the reaction, in the asymptotic limit one of the isomers will emerge as the winner, i.e., it will be present as the majority, and the other isomer will perish, which we refer to as the loser. Instead of monitoring the average domain size of both isomers, we have studied the kinetics of both of them separately.

Our results show that for higher reaction probability p_r, the dynamics of the system resembles ferromagnetic ordering throughout the evolution. There one observes the usual scaling of the two-point equal-time correlation function $C(r, t)$ and the structure factor $S(k, t)$. As p_r decreases, these quantities show a signature of the strong interplay between the segregation dynamics and the reaction dynamics; thereby the overall scaling picture does not hold anymore. For very low p_r, instead one observes an early-time scaling that resembles the conserved dynamics due to phase segregation. However, the universal Porod-tail behavior of $S(k, t) \sim k^{-3}$ remains unaffected for any choice of p_r.

While for large p_r the time dependence of the average domain size of the winner $\ell_1(t)$ and loser $\ell_2(t)$ show behavior consistent with ferromagnetic ordering, with decrease of p_r the interplay of the conserved and nonconserved dynamics show up. In fact, one observes a crossover in the growth from an initial slow $\ell_1(t) \sim t^{1/7}$ behavior to the usual $\ell_1(t) \sim t^{1/2}$ growth at late times. The time dependence of $\ell_2(t)$ for small p_r also shows a similar crossover with initially growing similarly with the power law $\ell_2(t) \sim t^{1/7}$. Afterward, of course, $\ell_2(t)$ grows slower than $\ell_2(t) \sim t^{1/2}$. At very late times, $\ell_2(t)$ starts to decay and asymptotically almost vanishes. We have provided a heuristics to explain the surprisingly slow growth $\sim t^{1/7}$ in the early-time regime. Nonetheless, a proper theoretical understanding of this phenomenon is still required.

The observation of the crossover in the growth prompted us to also calculate a crossover time τ_s from the time dependence of the difference between average domain size of the winner and loser, which at late times grows as $\ell_1 - \ell_2 \sim t$. Our data for τ_s as a function of p_r appear to follow the power-law scaling $\tau_s \sim p_r^{-x}$, where we obtained $x = 1.05$, almost independent of temperature. The crossover time τ_s also appears to be independent of temperature for fixed values of p_r.

A facile adaptation of the methods presented here would be to consider a more complex reaction involving more than two species, for which MC simulation of an analogous q-state

Potts model seems to be an automatic choice [62–64]. In the future, it would also be interesting to study the effect of such interplay of phase segregation and interconversion reaction on the other aspect of nonequilibrium dynamics of phase transition, i.e., aging and related scaling [65–67]. Given recent growing interest in nonequilibrium dynamics of long-range systems, it would certainly be worth investigating this interplay of conserved and nonconserved dynamics using the long-range Ising model with power-law interaction [18–21,68,69]. Lastly, to invoke more real effects of modeling such a system, it would be challenging to construct a similar model where the reaction is happening in solutions. For that, one needs to perform MD simulations of a fluidlike system where the role of hydrodynamics has to be taken into account [70,71].

ACKNOWLEDGMENT

The work was funded by the Science and Engineering Research Board (SERB), Govt. of India through a Ramanujan Fellowship (File No. RJF/2021/000044).

[1] A. J. Bray, Theory of phase-ordering kinetics, Adv. Phys. **51**, 481 (2002).
[2] *Kinetics of Phase Transitions*, edited by S. Puri and V. Wadhawan (CRC Press, Boca Raton, 2009).
[3] H. E. Stanley, *Introduction to Phase Transitions and Critical Phenomena* (Clarendon Press, Oxford, 1971).
[4] M. E. Fisher, The renormalization group in the theory of critical behavior, Rev. Mod. Phys. **46**, 597 (1974).
[5] P. C. Hohenberg and B. I. Halperin, Theory of dynamic critical phenomena, Rev. Mod. Phys. **49**, 435 (1977).
[6] *Phase Transitions and Critical Phenomena*, edited by C. Domb, M. S. Green, and J. L. Lebowtiz (Academic Press, New York, 1972-2001), Vols. 1–20.
[7] E. D. Siggia, Late stages of spinodal decomposition in binary mixtures, Phys. Rev. A **20**, 595 (1979).
[8] H. Furukawa, Effect of inertia on droplet growth in a fluid, Phys. Rev. A **31**, 1103 (1985).
[9] H. Furukawa, Turbulent growth of percolated droplets in phase-separating fluids, Phys. Rev. A **36**, 2288 (1987).
[10] S. M. Allen and J. W. Cahn, A microscopic theory for antiphase boundary motion and its application to antiphase domain coarsening, Acta Metall. **27**, 1085 (1979).
[11] I. M. Lifshitz and V. V. Slyozov, The kinetics of precipitation from supersaturated solid solutions, J. Phys. Chem. Solids **19**, 35 (1961).
[12] I. M. Lifshitz, Kinetics of ordering during second-order phase transitions, Sov. Phys. JETP **15**, 939 (1962).
[13] J. F. Marko and G. T. Barkema, Phase ordering in the Ising model with conserved spin, Phys. Rev. E **52**, 2522 (1995).
[14] J. G. Amar, F. E. Sullivan, and R. D. Mountain, Monte Carlo study of growth in the two-dimensional spin-exchange kinetic Ising model, Phys. Rev. B **37**, 196 (1988).
[15] S. Majumder and S. K. Das, Domain coarsening in two dimensions: Conserved dynamics and finite-size scaling, Phys. Rev. E **81**, 050102(R) (2010).
[16] S. Majumder and S. K. Das, Diffusive domain coarsening: Early time dynamics and finite-size effects, Phys. Rev. E **84**, 021110 (2011).
[17] S. Majumder and S. K. Das, Temperature and composition dependence of kinetics of phase separation in solid binary mixtures, Phys. Chem. Chem. Phys. **15**, 13209 (2013).
[18] H. Christiansen, S. Majumder, and W. Janke, Phase ordering kinetics of the long-range Ising model, Phys. Rev. E **99**, 011301(R) (2019).
[19] H. Christiansen, S. Majumder, M. Henkel, and W. Janke, Aging in the long-range Ising model, Phys. Rev. Lett. **125**, 180601 (2020).
[20] H. Christiansen, S. Majumder, and W. Janke, Zero-temperature coarsening in the two-dimensional long-range Ising model, Phys. Rev. E **103**, 052122 (2021).
[21] F. Müller, H. Christiansen, and W. Janke, Phase-separation kinetics in the two-dimensional long-range Ising model, Phys. Rev. Lett. **129**, 240601 (2022).
[22] A. D. McNaught and A Wilkinson, *Compendium of Chemical Terminology* (Blackwell Science, Oxford, 1997), Vol. 1669.
[23] K. Soai, T. Shibata, H. Morioka, and K. Choji, Asymmetric autocatalysis and amplification of enantiomeric excess of a chiral molecule, Nature (London) **378**, 767 (1995).
[24] T. Shibata, K. Choji, T. Hayase, Y. Aizu, and K. Soai, Asymmetric autocatalytic reaction of 3-quinolylalkanol with amplification of enantiomeric excess, Chem. Commun. **10**, 1235 (1996).
[25] T. Shibata, H. Morioka, T. Hayase, K. Choji, and K. Soai, Highly enantioselective catalytic asymmetric automultiplication of chiral pyrimidyl alcohol, J. Am. Chem. Soc. **118**, 471 (1996).
[26] Q. Tran-Cong and A. Harada, Reaction-induced ordering phenomena in binary polymer mixtures, Phys. Rev. Lett. **76**, 1162 (1996).
[27] Qui Tran-Cong, T. Ohta, and O. Urakawa, Soft-mode suppression in the phase separation of binary polymer mixtures driven by a reversible chemical reaction, Phys. Rev. E **56**, R59 (1997).
[28] T. Ohta, O. Urakawa, and Q. Tran-Cong, Phase separation of binary polymer blends driven by photoisomerization: An example for a wavelength-selection process in polymers, Macromolecules **31**, 6845 (1998).
[29] C. Viedma, Chiral symmetry breaking during crystallization: Complete chiral purity induced by nonlinear autocatalysis and recycling, Phys. Rev. Lett. **94**, 065504 (2005).
[30] T. G. Lombardo, F. H. Stillinger, and P. G. Debenedetti, Thermodynamic mechanism for solution phase chiral amplification via a lattice model, Proc. Natl. Acad. Sci. USA **106**, 15131 (2009).
[31] K. Blom and A. Godec, Criticality in cell adhesion, Phys. Rev. X **11**, 031067 (2021).
[32] F. Barret and N. Torri, Hydrodynamic limit of the Schelling model with spontaneous Glauber and Kawasaki dynamics, Electron. J. Probab. **29**, 1 (2024).

[33] T. C. Schelling, Dynamic models of segregation, J. Math. Soc. **1**, 143 (1971).
[34] D. Zwicker, R. Seyboldt, C. A. Weber, A. A. Hyman, and F. Jülicher, Growth and division of active droplets provides a model for protocells, Nat. Phys. **13**, 408 (2017).
[35] C. A. Weber, D. Zwicker, F. Jülicher, and C. F. Lee, Physics of active emulsions, Rep. Prog. Phys. **82**, 064601 (2019).
[36] N. Ziethen, J. Kirschbaum, and D. Zwicker, Nucleation of chemically active droplets, Phys. Rev. Lett. **130**, 248201 (2023).
[37] S. C. Glotzer, D. Stauffer, and N. Jan, Monte Carlo simulations of phase separation in chemically reactive binary mixtures, Phys. Rev. Lett. **72**, 4109 (1994).
[38] S. Puri and H. L. Frisch, Segregation dynamics of binary mixtures with simple chemical reactions, J. Phys. A **27**, 6027 (1994).
[39] S. C. Glotzer, E. A. Di Marzio, and M. Muthukumar, Reaction-controlled morphology of phase-separating mixtures, Phys. Rev. Lett. **74**, 2034 (1995).
[40] A. Singh, S. Puri, and C. Dasgupta, Growth kinetics of nanoclusters in solution, J. Phys. Chem. B **116**, 4519 (2012).
[41] N. A. Shumovskyi, T. J. Longo, S. V. Buldyrev, and M. A. Anisimov, Phase amplification in spinodal decomposition of immiscible fluids with interconversion of species, Phys. Rev. E **103**, L060101 (2021).
[42] T. J. Longo and M. A. Anisimov, Phase transitions affected by natural and forceful molecular interconversion, J. Chem. Phys. **156**, 084502 (2022).
[43] T. J. Longo, N. A. Shumovskyi, B. Uralcan, S. V. Buldyrev, M. A. Anisimov, and P. G. Debenedetti, Formation of dissipative structures in microscopic models of mixtures with species interconversion, Proc. Natl. Acad. Sci. USA **120**, e2215012120 (2023).
[44] S. Thwal and S. Majumder, Segregation disrupts the Arrhenius behavior of an isomerization reaction, Phys. Rev. E **109**, 034119 (2024).
[45] R. J. Glauber, Time-dependent statistics of the Ising model, J. Math. Phys. **4**, 294 (1963).
[46] K. Kawasaki, Diffusion constants near the critical point for time-dependent Ising models. I, Phys. Rev. **145**, 224 (1966).
[47] S. Majumder, Disentangling growth and decay of domains during phase ordering, Phys. Rev. E **107**, 034130 (2023).
[48] L. Onsager, Crystal statistics. I. A two-dimensional model with an order-disorder transition, Phys. Rev. **65**, 117 (1944).
[49] M. E. J. Newman and G. T. Barkema, *Monte Carlo Methods in Statistical Physics* (Oxford University Press, Oxford, 1999).
[50] D. Landau and K. Binder, *A Guide to Monte Carlo Simulations in Statistical Physics* (Cambridge University Press, Cambridge, 2021).
[51] B. C. S. Grandi and W. Figueiredo, Monte Carlo simulation of an Ising antiferromagnet with competing Glauber and Kawasaki dynamics, Phys. Rev. E **56**, 5240 (1997).
[52] Z.-F. Huang, B.-L. Gu, and Y. Tang, Scaling for domain growth in the Ising model with competing dynamics, Phys. Rev. E **58**, 7126 (1998).
[53] S. Artz and S. Trimper, Competing Glauber and Kawasaki dynamics, Int. J. Mod. Phys. B **12**, 2385 (1998).
[54] A. Szolnoki, Phase transitions in the kinetic Ising model with competing dynamics, Phys. Rev. E **62**, 7466 (2000).
[55] G. O. Berim and E. Ruckenstein, Phase transformation in a lattice system in the presence of spin-exchange dynamics, J. Chem. Phys. **120**, 2851 (2004).
[56] G. O. Berim and E. Ruckenstein, Kinetics of phase transformation on a Bethe lattice in the presence of spin exchange, J. Chem. Phys. **120**, 9800 (2004).
[57] G. Porod, Die Röntgenkleinwinkelstreuung von dichtgepackten kolloiden Systemen, Kolloid-Zeitschrift **124**, 83 (1951).
[58] G. Porod, General theory, in *Small Angle X-ray Scattering*, edited by O. Glatter and O. Kratky (Acdemic Press, London, 1982), pp. 17–35.
[59] J. Olejarz, P. L. Krapivsky, and S. Redner, Zero-temperature coarsening in the 2D Potts model, J. Stat. Mech.: Theory Exp. (2013) P06018.
[60] B. Efron, *The Jackknife, the Bootstrap and Other Resampling Plans* (Society for Industrial and Applied Mathematics, Philadelphia, 1982).
[61] V. Spirin, P. L. Krapivsky, and S. Redner, Fate of zero-temperature Ising ferromagnets, Phys. Rev. E **63**, 036118 (2001).
[62] F.-Y. Wu, The Potts model, Rev. Mod. Phys. **54**, 235 (1982).
[63] S. Majumder, S. K. Das, and W. Janke, Universal finite-size scaling function for kinetics of phase separation in mixtures with varying number of components, Phys. Rev. E **98**, 042142 (2018).
[64] W. Janke, S. Majumder, and S. K. Das, Universal finite-size scaling function for coarsening in the Potts model with conserved dynamics, J. Phys.: Conf. Ser. **2122**, 012009 (2021).
[65] M. Henkel and M. Pleimling, *Non-Equilibrium Phase Transitions: Ageing and Dynamical Scaling far from Equilibrium* (Springer, Heidelberg, 2010), Vol. 2.
[66] J. Midya, S. Majumder, and S. K. Das, Aging in ferromagnetic ordering: Full decay and finite-size scaling of autocorrelation, J. Phys.: Condens. Matter **26**, 452202 (2014).
[67] J. Midya, S. Majumder, and S. K. Das, Dimensionality dependence of aging in kinetics of diffusive phase separation: Behavior of order-parameter autocorrelation, Phys. Rev. E **92**, 022124 (2015).
[68] F. Müller, H. Christiansen, S. Schnabel, and W. Janke, Fast, hierarchical, and adaptive algorithm for metropolis Monte Carlo simulations of long-range interacting systems, Phys. Rev. X **13**, 031006 (2023).
[69] W. Janke, H. Christiansen, and S. Majumder, The role of magnetization in phase-ordering kinetics of the short-range and long-range Ising model, Eur. Phys. J.: Spec. Top. **232**, 1693 (2023).
[70] S. Majumder and Subir K Das, Universality in fluid domain coarsening: The case of vapor-liquid transition, Europhys. Lett. **95**, 46002 (2011).
[71] S. Majumder and S. K. Das, Effects of density conservation and hydrodynamics on aging in nonequilibrium processes, Phys. Rev. Lett. **111**, 055503 (2013).